Vectorial optical field reconstruction by attosecond spatial interferometry

P. Carpeggiani[1,2†], M. Reduzzi[1,2†], A. Comby[1†], H. Ahmadi[1,3], S. Kühn[4], F. Calegari[2,5,6], M. Nisoli[1,2], F. Frassetto[7], L. Poletto[7], D. Hoff[8], J. Ullrich[9], C. D. Schröter[10], R. Moshammer[10], G. G. Paulus[8] and G. Sansone[1,2,4,11*]

An electrical pulse E(*t*) is defined completely by its time-dependent amplitude and polarization direction. For optical pulses the manipulation and characterization of the light polarization state is fundamental because of its relevance in several scientific and technological fields. In this work, we demonstrate the complete temporal reconstruction of the electric field of few-cycle pulses with a complex time-dependent polarization. Our experimental approach is based on extreme ultraviolet interferometry with isolated attosecond pulses and on the demonstration that the motion of an attosecond electron wave packet is sensitive to perturbing fields only along the direction of its motion. By exploiting the sensitivity of interferometric techniques and by controlling the emission and acceleration direction of the wave packet, pulses with energies as low as a few hundreds of nanojoules can be reconstructed. Our approach reveals the possibility to characterize completely the electric field of the pulses typically used in visible pump–probe spectroscopy.

The complete characterization of optical pulses requires that it is possible to sample in time oscillating electric fields on a sub-femtosecond timescale. In the past decade, the development of attosecond science and technology has made available the technological tools towards this goal[1–3]. In general, the electric field $\mathbf{E}(t)$ is a vector quantity and the measurement of the (time-dependent) polarization is required for its complete reconstruction. The polarization state of the radiation is a key parameter in the light–matter interaction, as it determines the selection rules in the photoexcitation and photoionization of atoms and molecules, and spin properties of photoelectrons emitted from surfaces. Moreover, polarization shaping and synthetization of complex time-dependent polarizations are widely adopted schemes to control laser–matter interaction at high intensities[4,5], at the nanoscale level[6] and for the optimal control of quantum systems[7].

An electric field with a time-dependent polarization can be retrieved by measuring its components along two (perpendicular) directions. For ultrashort pulses that approach the single-cycle regime[8], the rotation of the polarization axis through wave plates can introduce distortions because of the large spectral bandwidth and higher-order phase-dispersion terms. Therefore, the characterization along these two directions should avoid the use of such additional dispersive elements.

A technique able to characterize weak probe pulses fully with the energy of a few tens or hundreds of nanojoules is also desirable. In this way, the full reconstruction of electric fields would not be limited to intense pulses[9], but it could be extended to the probe pulses typically used in visible and infrared pump–probe spectroscopy.

Two complementary approaches have been demonstrated so far for the complete characterization of optical waveforms: the attosecond streak camera[10,11] and the petahertz optical oscilloscope[12]. Electric fields with linear[13] and time-dependent polarization[14] were retrieved using the first approach, which, however, requires the use of intense fields. However, the second technique introduces a systematic distortion of the reconstructed waveform because of the non-collinear geometry[12].

Extreme ultraviolet (XUV) spatial interferometry

In our experimental approach, we take advantage of XUV spatial interferometry driven by isolated attosecond pulses to demonstrate the full reconstruction of unknown fields characterized by a complex polarization pattern. XUV spatial interferometry of high-order harmonic sources has been demonstrated already with trains of attosecond pulses for the investigation of plasma[15] and molecular[16] dynamics. In these approaches, one XUV pulse acts as a reference, whereas the characteristics (phase or amplitude) of the second one are modified by the ongoing dynamics.

The application of XUV interferometry for the reconstruction of optical pulses is presented in Fig. 1a: two coherent intense driving fields are focused in two closely spaced focal spots (A and B), at which two attosecond electronic wave packets are released by tunnel ionization into the continuum and accelerated. When the electric field drives back the wave packets, two closely spaced coherent isolated attosecond pulses are generated upon the recombination of the electrons with the ground state of the parent ions. The polarization direction of the isolated attosecond pulses is linked to the direction of motion of the electronic wave packets (the x direction in Fig. 1a), which is determined by the direction of polarization of the driving field. The two XUV pulses interfere in the far field along the vertical direction, whereas the spectra are dispersed by a suitable optical set-up in the perpendicular direction (Fig. 1b). The unknown perturbing optical pulse, $\mathbf{E}_{\mathrm{unk}}$, is overlapped in one

[1]Dipartimento di Fisica, Politecnico Piazza Leonardo da Vinci 32, 20133 Milano, Italy. [2]IFN-CNR, Piazza Leonardo da Vinci 32, 20133 Milano Italy. [3]Department of Physical Chemistry, School of Chemistry, College of Science, University of Tehran, PO Box 14155-6455 Tehran, Iran. [4]ELI-ALPS, ELI-Hu Kft., Dugonics ter 13, H-6720 Szeged, Hungary. [5]Deutsches Elektronen-Synchrotron, Notkestrasse 85, Hamburg 22607, Germany. [6]Physics Department, University of Hamburg, Luruper Chaussee 149, 22761 Hamburg, Germany. [7]Institute of Photonics and Nanotechnologies, CNR via Trasea 7, 35131 Padova Italy. [8]Institut für Optik und Quantenelektronik, Friedrich-Schiller-Universität Jena, Max-Wien-Platz 1, 07743 Jena, Germany. [9]Physikalisch-Technische Bundesanstalt, Bundesallee 100, 38116 Braunschweig, Germany. [10]Max-Planck-Institut für Kernphysik, Saupfercheckweg 1, 69117 Heidelberg, Germany. [11]Physikalisches Institut, Albert-Ludwigs-Universität Freiburg, 79106 Freiburg, Germany. [†]These authors contributed equally to this work. *e-mail: giuseppe.sansone@physik.uni-freiburg.de

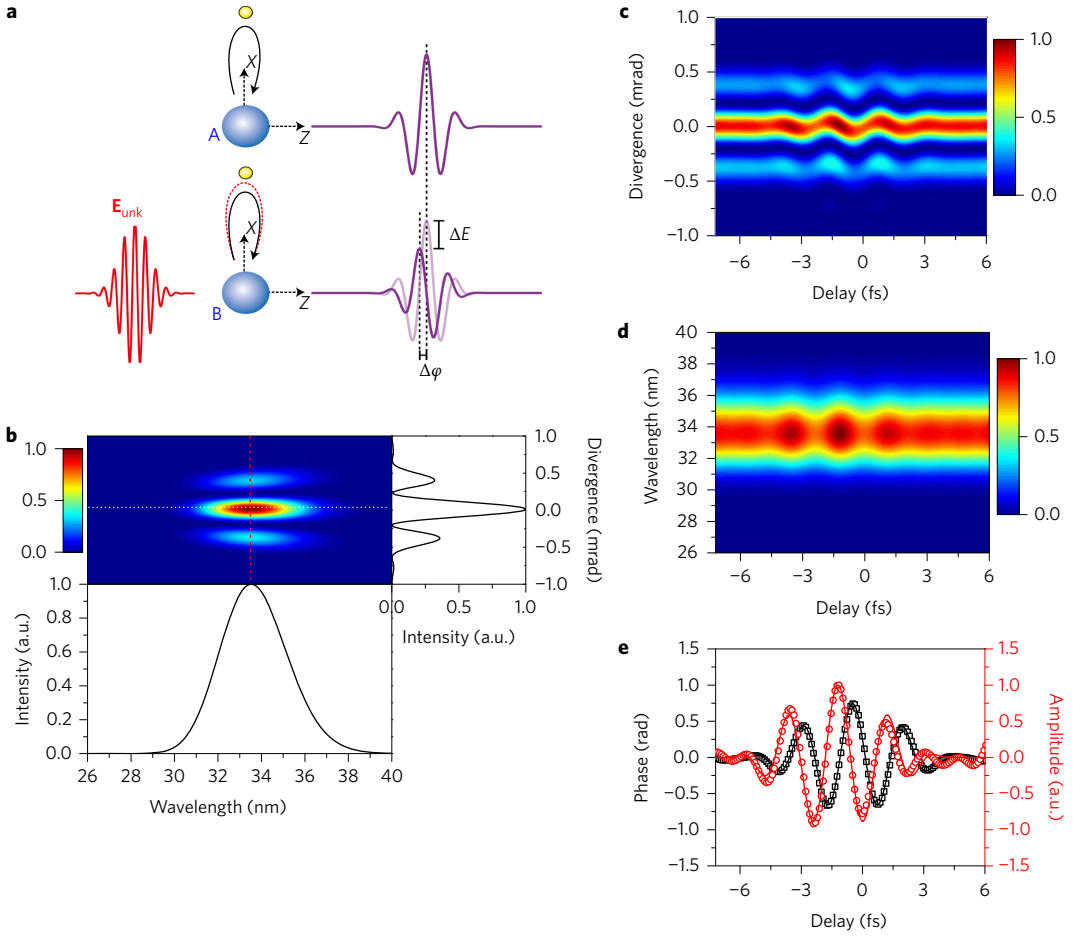

Figure 1 | XUV spatial interferometry with isolated attosecond pulses. a, Two electronic wave packets, on recollision, lead to the generation of two coherent isolated attosecond pulses, which interfere in the far field. A weak probe pulse, $\mathbf{E}_{unk}$, perturbs the amplitude (ΔE) and phase ($\Delta\varphi$) of one of the two attosecond pulses. **b**, Simulated XUV interference pattern on the output plane of an XUV spectrometer. The right and lower panels show the projections along the vertical (red dashed line) and horizontal (white dashed line) directions, which correspond to the divergence and the spectrum of the XUV interference pattern, respectively. The parameters of the experiment were used in the simulations (Supplementary Information). **c**,**d**, Dependence of the divergence (**c**) and of the spectrum (**d**) of the simulated XUV interference pattern on the delay τ. **e**, Electric fields retrieved from the amplitude (red circles, arbitrary units) and the phase (black squares) using a Fourier analysis of the oscillations of Fig. 1c (Supplementary Information). The time difference between the two reconstructed fields is about a quarter of an optical cycle. The field used in the simulation is shown by solid lines (red and black). The input fields have been shifted and normalized to match the reconstructed ones. Parameters used in the simulations: full-width at half-maximum (FWHM) = 5 fs, $\lambda = 744$ nm, $I = 3.5 \times 10^{14}$ W cm^{-2} and CEP = 0 for the driving field; FWHM = 5 fs, $\lambda = 744$ nm, $I = 3.5 \times 10^{10}$ W cm^{-2} and CEP = 0 for the unknown field.

of the two focal spots. The weak field perturbs the generation of XUV radiation, which leads to a modulation in the amplitude (ΔE) and phase ($\Delta\varphi$) of one of the two isolated attosecond pulses. This modulation is imprinted in the strength (amplitude) and position (phase) of the interference fringes (Supplementary Movie 1), and it is determined by the instantaneous unknown field during the motion of the electronic wave packet[12]. Indeed, ΔE and $\Delta\varphi$ are related to the imaginary and real part of the phase accumulated by the electron wave packet in the continuum (S)[17], which is determined by the ionization (t_{ion}) and recombination (t_{rec}) times, and by the total field experienced by the electron wave packet in the continuum. We have verified that these three quantities depend linearly on the amplitude of the unknown field (in a suitable intensity range, as discussed below).

By changing the arrival time τ of the pulse, the fringe position and the total signal of the XUV spectrum oscillate, as shown in Fig. 1c,d, respectively. The electric field of the perturbing field can be reconstructed from either the amplitude or the phase of the oscillation of the interference pattern, as shown in Fig. 1e, which reports the input field (solid lines) and the electric field reconstructed from the amplitude and phase of the oscillations. The input field was shifted in time and normalized to match the reconstructed fields. The amplitude modulation of the interference pattern can be attributed to the variation of the ionization probability because of the presence of the unknown field. Therefore, the field reconstructed from this modulation corresponds to the unknown field at the ionization instant. However, the phase modulation of the interference pattern is caused by the variation of the phase accumulated by the electron wave packet between the ionization and recombination instants. The reconstructed field corresponds to an average value of the unknown field between these two instants. For this reason, the reconstructions from the amplitude and phase modulations present a temporal offset, as shown in Fig. 1e.

We have verified that the effect on the phase of the interference pattern scales linearly with the electric field for peak intensities between $I = 5.8 \times 10^{8}$ W cm^{-2} and $I = 9 \times 10^{12}$ W cm^{-2}. The effect on the amplitude of the modulation is linear in a

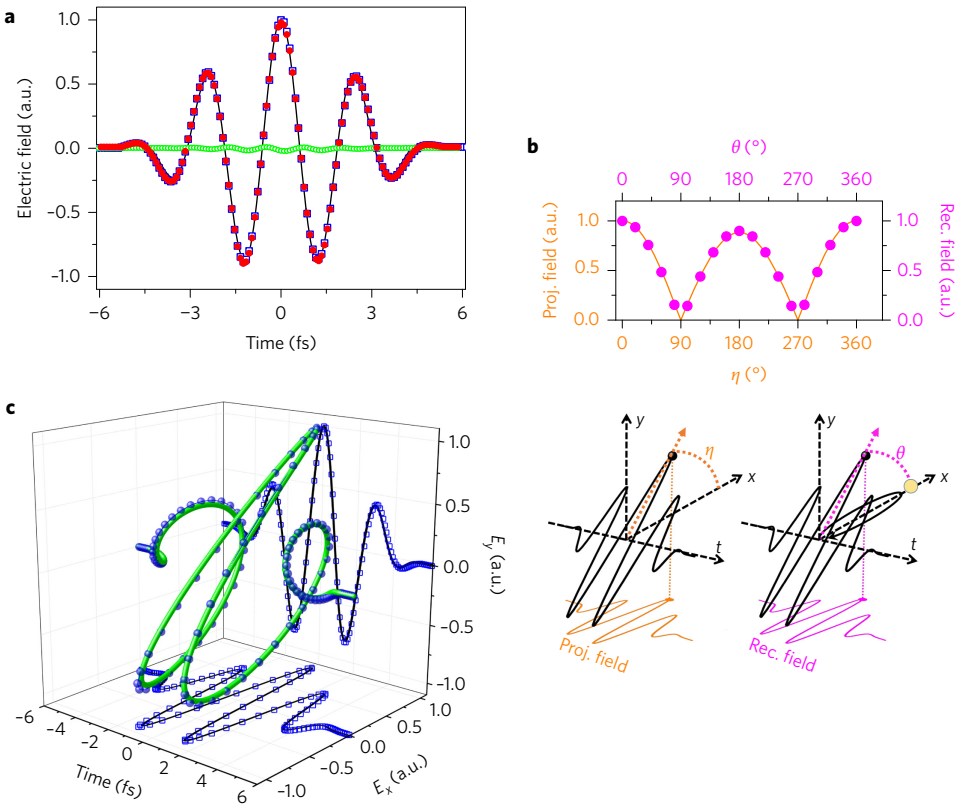

Figure 2 | Single-electron recollision as a time-gated directional field detector. a, Simulated (black line) and reconstructed electric field in the case of linear polarizations parallel (blue open squares) and perpendicular (green open circles) to the motion of the electronic wave packet, and in the case of circular polarization (red filled circles). Parameters of the simulation: FWHM = 4 fs, $\lambda = 600$ nm and CEP = 0. **b**, The maximum amplitude of the projection of the electric field of a linearly polarized pulse along the reference x direction as a function of the relative angle η between this direction and the polarization axis of the field (orange line), and the maximum amplitude of the reconstructed field as a function of the relative angle θ between the motion of the electronic wave packet and the polarization axis of the field (magenta points). **c**, Simulated (green solid line) and retrieved (blue spheres) electric fields for a pulse with a time-dependent polarization state. The projections along the x and y directions are shown for the input (black lines; x direction FWHM = 4 fs, $\lambda = 600$ nm, $I = 3.5 \times 10^{10}$ W cm^{-2} and CEP = 0; y direction FWHM = 4 fs, $\lambda = 744$ nm, $I = 3.5 \times 10^{10}$ W cm^{-2} and CEP = 0) and for the reconstructed (blue open squares) fields. Proj., projected; Rec., reconstructed.

smaller intensity range (up to about $I = 5 \times 10^{11}$ W cm^{-2}). This difference can be attributed to the exponential dependence of the tunnelling ionization rate on the electric field, which limits the intensity range for the linear dependence on the unknown field. For this reason, in the following we focus on the electric fields reconstructed from the phase of the interference pattern.

We have also verified that pulses with a carrier wavelength as short as 200 nm can be reproduced with an error between 5 and 15% (evaluated on the single reconstructed electric field value), depending on the duration of the unknown pulse.

Attosecond electron dynamics as a field detector

The strength of the effect and, therefore, the reconstruction of the electric field strongly depends on the relative orientation between the direction of the electronic motion (determined by the direction of polarization of the driving field) and the instantaneous polarization direction of the unknown field. This is demonstrated in Fig. 2a, which shows a linearly polarized field (continuous black line) and the reconstructed fields in the case of polarization parallel (blue open squares) and perpendicular (green open circles) to the motion of the electronic wave packet. The reconstruction of a (almost) zero field in the perpendicular case reveals that the electronic motion is (almost) unaffected by the unknown field in this configuration. This can be explained by observing that the phase S accumulated by the electronic wave packet depends on the integral of the kinetic energy between the ionization and recombination instants[17]:

$$S \propto \int_{t_{ion}}^{t_{rec}} [\mathbf{p}_s + e\mathbf{A}_{dr}(t) + e\mathbf{A}_{unk}(t)]^2 dt \simeq \int_{t_{ion}}^{t_{rec}} [\mathbf{p}_s + e\mathbf{A}_{dr}(t)]^2 + 2[\mathbf{p}_s + e\mathbf{A}_{dr}(t)]e\mathbf{A}_{unk}(t) dt \quad (1)$$

where e, $\mathbf{p}_s$, $\mathbf{A}_{dr}(t)$ and $\mathbf{A}_{unk}(t)$ indicate the electron charge, stationary momentum and the vector potential of the driving and unknown fields, respectively. The driving field steers the motion of the electronic wave packet along its polarization direction ($\mathbf{p}_s$ is parallel to $\mathbf{A}_{dr}(t)$ with an excellent approximation), which thus makes negligible the contribution of the second term of equation (1) and the influence of the unknown perturbing field when the two pulses are perpendicularly polarized. This conclusion holds true up to intensities for which the unknown field can no longer be considered a perturbation of the driving one. As the electronic motion is sensitive to the parallel but not the perpendicular perturbation, the phase and amplitude of the isolated attosecond pulse encode information only on the projection of the instantaneous electric field along the direction of motion. For the reconstruction of the unknown field, the electronic dynamics acts as a time-gated directional field detector, which is sensitive only to the field component along its main axis (which coincides with the direction of motion of the electron) within a time-gating window. Owing to

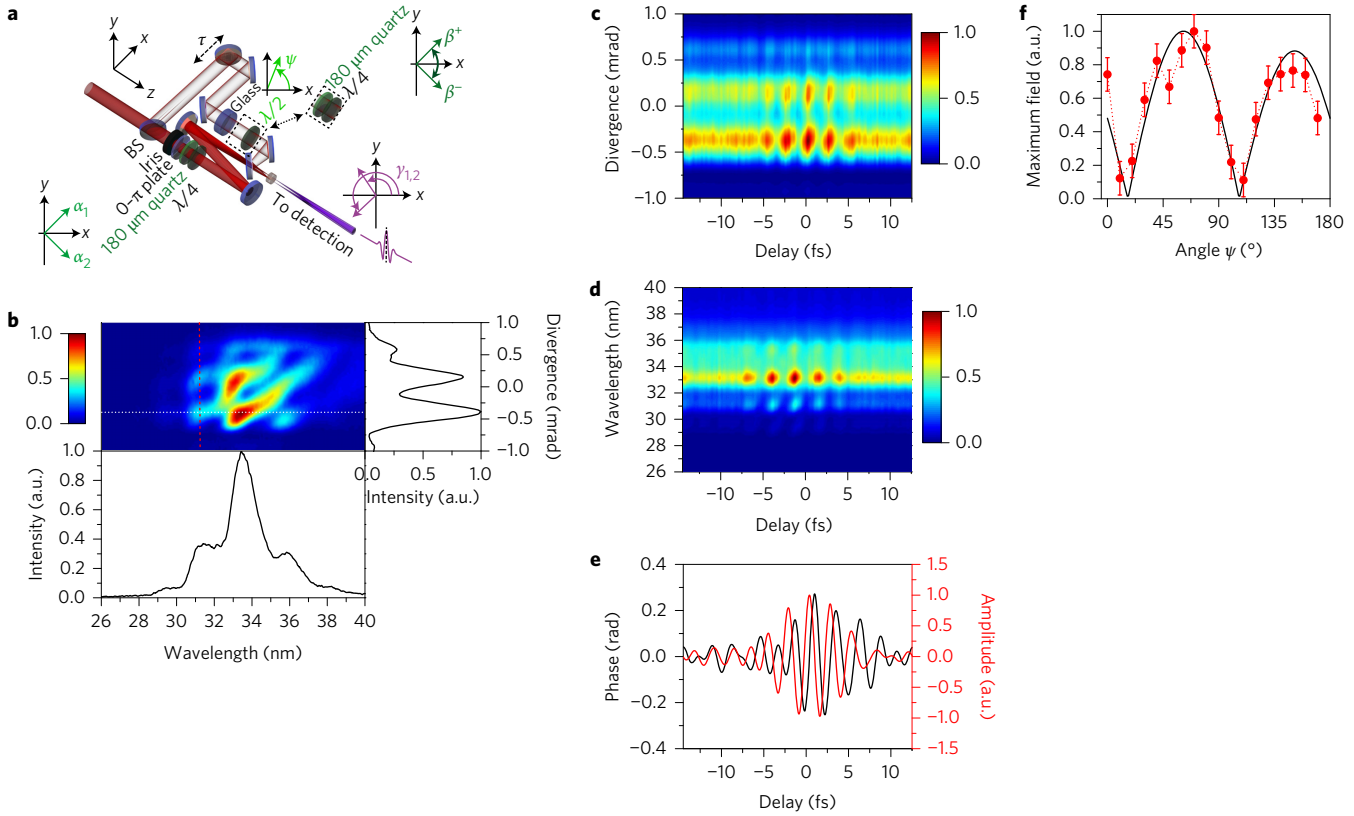

Figure 3 | Experimental set-up and reconstruction of linearly polarized few-cycle pulses. a, Experimental set-up. A beamsplitter (BS) divided the incoming beam in the driving and the unknown perturbing pulses. The intensity of the field that drives the high-order harmonic generation process was adjusted by an iris. The binary 0–π plate introduced a π-phase shift that led to two coherent foci in the focal plane of the 150 mm focal-length focusing mirror. The polarization of the driving pulse was modulated in time by a PG unit (delay plate with a thickness $d = 180$ μm and zero-order quarter-wave plate). The unknown field is collinearly recombined using a drilled mirror. **b**, Experimental XUV interference pattern measured in the far field. The right and lower panels show the projections along the vertical (red dashed line) and horizontal (white dashed line) directions, which correspond to the divergence and the spectrum of the XUV interference pattern, respectively. **c**,**d**, Dependence of the divergence (**c**) and of the spectrum (**d**) of the experimental XUV interference pattern on the delay τ. **e**, Electric fields retrieved from the amplitude (red line) and the phase (black line) using a Fourier analysis of the oscillations of **c**. **f**, Evolution of the experimental maximum electric field as a function of the rotation angle ψ of the $\lambda/2$ wave plate on the unknown field (red circles). The black line indicates the expected maximum of the electric field. The error bars were estimated as the amplitude of the noise on the reconstruction for delays much larger than the pulse duration.

the dynamics of the electronic wave packet in the continuum, the duration of the gate amounts to a few hundreds of attoseconds.

This conclusion is illustrated in Fig. 2b, which shows the maximum of the projection of the linearly polarized field of Fig. 2a, along a reference direction (x), as a function of the angle η between this direction and the polarization axis of the field. As expected, the curve evolves as $|\cos(\eta)|$ (orange line), with a small difference between $\eta = 0°$ and $\eta = 180°$ because of the asymmetry of the few-cycle field.

The maximum field of the pulse, reconstructed by the analysis of the evolution of the interference pattern (magenta points) as a function of the angle θ between the direction of the electronic wave packet and the perturbing field, matches perfectly the evolution of the maximum of the projected field. We also verified that both the maximum amplitudes and the evolution in time of the complete field are well reproduced for all relative angles.

The component of the electric field perpendicular to the electronic motion does not affect the reconstruction for a generic polarization state of the unknown pulse. This is demonstrated by the reconstruction of the field for a pulse with a circular polarization (Fig. 2a, red filled circles). Also, in this case the reconstructed field is given by the projection of the vectorial field along the axis of the time-gated directional field detector. A similar conclusion holds true for elliptically polarized pulses.

These observations suggest the possibility of the characterization of pulses with a complex time-dependent polarization, by applying the reconstruction along two (perpendicular) polarization directions of the isolated attosecond pulses. As an example (Fig. 2c), we considered two perpendicularly polarized few-cycle pulses with different carrier frequencies. Owing to the different periods of oscillation, the polarization state of the total field varies from circular on the edges of the pulses (with opposite helicities) to linear in the centre. The reconstruction of the pulse along the perpendicular directions (x and y, blue squares in Fig. 2c) follows perfectly the input fields, and thus gives access to the complete characterization of the vectorial field.

Full reconstruction of linearly polarized electric fields

In the experimental set-up (Fig. 3a), we used the polarization gating (PG) technique to implement XUV spatial interferometry with isolated attosecond pulses[18,19]. The few-cycle pulses passed through a binary plate, which imposed a π-phase difference between the lower and upper halves of the beam[16]. In the focus, this phase difference caused two closely spaced coherent focal spots, which were the source points of the two isolated attosecond pulses. The far-field interference pattern of the two XUV pulses is presented in Fig. 3b. Clear interference fringes were observed in the vertical direction, whereas the spectrum was dispersed in the horizontal direction by a grazing incidence XUV spectrometer. The deviation of the

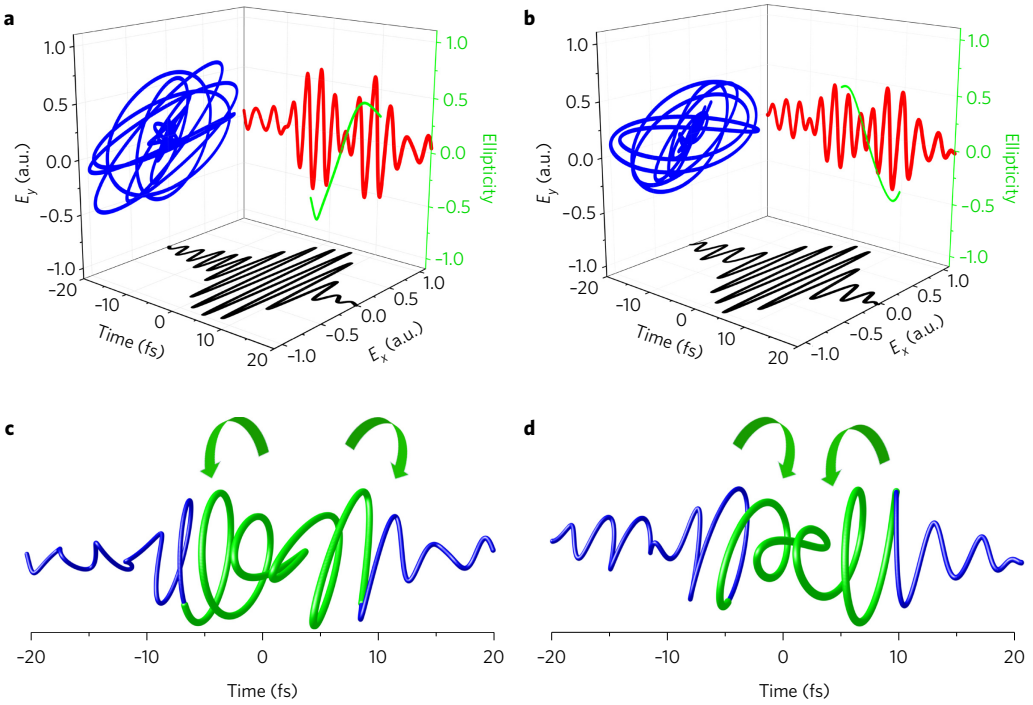

Figure 4 | Reconstruction of electric fields with time-dependent polarization. a,**b**, Reconstructed electric fields (E_x component, black solid line; E_y component, red solid line) projection in the plane x–y perpendicular to the propagation direction (blue solid line) and ellipticity (green solid line) for $\beta^+ = +45°$ (**a**) and $\beta^- = -45°$ (**b**). **c**,**d**, 3D representation of the two fields with time-dependent polarization for $\beta^+ = +45°$ (**c**) and $\beta^- = -45°$ (**d**). The arrows indicate the helicities for the two cases. The green sections correspond to the ellipticity variations shown in **a** and **b**.

interference fringes from the horizontal direction can be attributed to small misalignments in the grazing incidence spectrometer.

The unknown perturbing field $\mathbf{E}_{unk}$ (initially linearly polarized along the x direction) was overlapped with one of the two foci. In the experiment, we typically used unknown pulses with energies on the order of a few hundreds of nanojoule that correspond to intensities of about 10^{10}–10^{11} W cm^{-2}. A peak intensity as low as $\sim 10^9$ W cm^{-2} still produced a significant shift of the fringes (~0.1 rad), which could be measured experimentally with our set-up.

Figure 3c,d shows the divergence and the XUV signal as a function of the relative delay between the driving and perturbing fields, respectively. The delay dependences are in good agreement with the simulations presented in Fig. 1c,d (Supplementary Movie 2). The field retrieved from the amplitude and phase modulations is shown in Fig. 3e. These measurements demonstrate the reconstruction of few-cycle linearly polarized pulses using spatial interferometry based on isolated attosecond pulses. The robustness of the reconstruction was verified using different XUV wavelengths and different algorithms (Supplementary Information).

To demonstrate that the dynamics of the electronic wave packet is sensitive only to the weak field parallel to its motion, we measured the unknown field for different rotation angles ψ of a half-wave plate inserted in the beam path (Fig. 3a). The maxima of the reconstructed field (red circles in Fig. 3f) reproduced well the expected evolution ($|\cos(2\psi + \psi_0)|$, where ψ_0 is an offset angle), which confirms that the isolated attosecond pulse encodes information only on the perturbing field parallel to its polarization. The lowest intensity of the component of the perturbing field along the electronic direction used in Fig. 3f was estimated as $I_{unk} = 1.5 \times 10^9$ W cm^{-2}.

Electric field reconstruction with complex polarization

The reconstruction of complex vectorial fields requires the characterization of two (usually perpendicular) components. The PG technique offers a straightforward way to implement the reconstruction of optical fields along different directions, because the polarization directions $\gamma_{1,2}$ of the isolated attosecond pulses can be modified by simply rotating the angle of the first plate of the PG unit from $\alpha_1 = +45°$ to $\alpha_2 = -45°$ (Fig. 3a and the Supplementary Information). This approach presents the advantage that the axis of our directional-field-sensitive detector can be rotated without any additional dispersive optical element, distorting neither the driving field nor the perturbing field. By measuring the projections $E_1(t)$ and $E_2(t)$ of the vector field $\mathbf{E}_{unk}(t)$ along the two directions identified by γ_1 and γ_2, the two perpendicular components $E_x(t)$ and $E_y(t)$ can be reconstructed (Supplementary Information).

To demonstrate the full capability of the technique, we synthesized fields with a complex time-dependent polarization state by replacing the half-wave plate with a replica of the PG unit acting on the unknown pulse (Fig. 3a). The axis of the plates of this second PG unit were initially aligned along the polarization of the incoming linearly polarized field. By rotating the angle β of the first plate to $\beta^{\pm} = \pm 45°$, a sharp transition from circular (elliptical) to linear and back to circular (elliptical) is expected. For opposite values of β, the helicity of the transition is expected to reverse[20–22]. For each $\beta^{\pm}$ angle, two measurements for α_1 and α_2 were acquired. Figure 4a,b shows the x and y components of the vectorial electric field retrieved for β^+ and β^-, respectively, and the projection of the field in the x–y plane. The pulse was characterized by a complex time-dependent ellipticity (Fig. 4a,b), which evolves from elliptical (positive helicity) to linear and back to elliptical (negative helicity) for $\beta^+ = +45°$. The transition between different polarization states can be observed clearly in a three-dimensional (3D) representation of the fields, which evidences a rotation of the polarization vector clockwise (anticlockwise) on the leading (falling) edge of the pulse for β^+ (Fig. 4c)[23]. For β^-, the rotation directions are reversed (Fig. 4d), as expected.

Our approach also allows for the characterization of the carrier-envelope phase (CEP) of the field by analysing the variations of the electric field components in the time window of the linear polarization. The CEP was controlled by changing the amount of fused

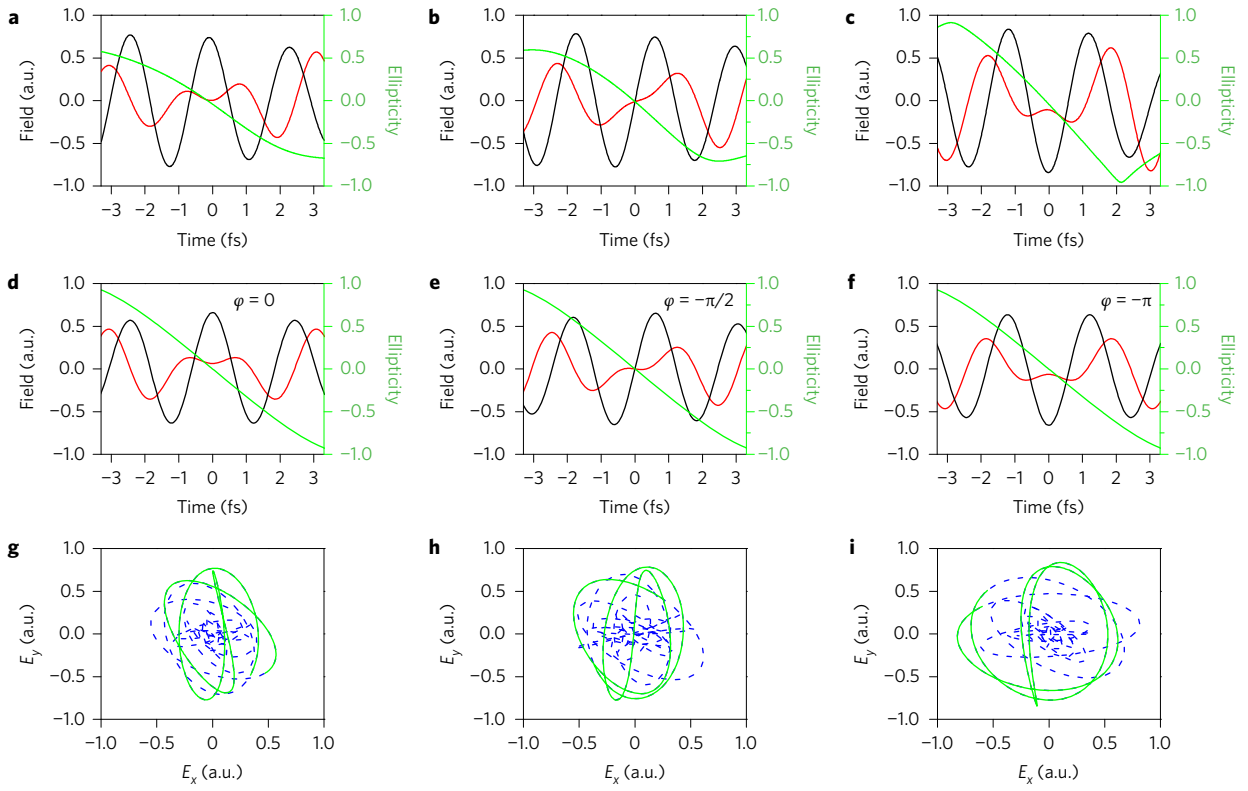

Figure 5 | Effect of the CEP in the temporal window of linear polarization. a–f, Measured (**a–c**) and simulated (**d–f**) electric fields (E_x component, black; E_y component, red) and ellipticities (green) for $\beta^+ = +45°$ and three CEPs, $\varphi = 0$ (**a**,**d**), $\varphi = -\pi/2$ (**b**,**e**) and $\varphi = -\pi$ (**c**,**f**). The ellipticity in the central temporal window (−3.3 fs to 3.3 fs) is highlighted in green. **g–i**, Experimental projection (blue dashed line) of the electric fields perpendicular to the propagation direction for the three CEPs, $\varphi = 0$ (**g**), $\varphi = -\pi/2$ (**h**) and $\varphi = -\pi$ (**i**). The green lines correspond to the projections in the temporal window (−3.3 fs to 3.3 fs) shown in **a–c**.

silica inserted in the beam path[24]. The reconstruction for three CEPs spaced by π/2 is shown in Fig. 5a–c. We can observe that the ellipticity is affected only slightly by the CEP as well as the component of the electric field along the x direction (apart from a shift in time). The minor component of the field, on the other hand, is strongly modified and even reversed for a π-phase shift (Fig. 5a,c). The simulations are shown in Fig. 5d–f, which report the field for the three CEPs, $\varphi = 0$, $\varphi = -\pi/2$ and $\varphi = -\pi$, respectively. The good matching between the simulations and the experiments allows a reliable determination of the CEP of the unknown field. The measured projection in the x–y plane is also reported in Fig. 5g–i. The field that corresponds to the time window of Fig. 5a–c is shown in green. The transition through a state of linear polarization is clearly visible, and it is evident that the projections are characterized by narrow (and opposite) regions of linear polarization for $\varphi = 0, -\pi$. This transition region becomes broader for intermediate CEPs ($\varphi = -\pi/2$). This periodic variation is in excellent agreement with the simulations (Supplementary Movie 3).

Conclusions

We have demonstrated the complete temporal characterization of the time-dependent amplitudes of the two components (including their CEPs) of a few-cycle pulse with a complex polarization state. The experimental approach is based on the implementation of spatial XUV interferometry and on the demonstration that the dynamics of a single-electron wave packet acts as an attosecond directionally sensitive field detector. These results reveal the possibility for the complete characterization of an optical field with a generic polarization state using an all-optical approach free from distortions. Combined with phase-sensitive detection techniques based on a lock-in amplifier, the sensitivity of the technique can be improved further, which provides new perspectives for the full characterization (amplitude, polarization, phase and CEP) of probe fields used in pump–probe spectroscopy. This approach offers the possibility to reconstruct the complete response (complex dielectric wavefunction) of metallic and nanostructured systems in the visible and infrared spectral range, in perfect analogy to time-domain spectroscopy for semiconductors in the terahertz domain.

Data availability. The data that support the plots within this paper and other findings of this study are available from the corresponding author upon reasonable request.

Received 8 October 2016; accepted 5 April 2017;
published online 29 May 2017; corrected after print 29 June 2017

References

1. Krausz, F. & Ivanov, M. Attosecond physics. *Rev. Mod. Phys.* **81,** 163–234 (2009).
2. Nisoli, M. & Sansone, G. New frontiers in attosecond science. *Prog. Quant. Electron.* **33,** 17–59 (2009).
3. Kapteyn, H., Cohen, O., Christov, I. & Murnane, M. Harnessing attosecond science in the quest for coherent X-rays. *Science* **317,** 775–778 (2007).
4. Corkum, P. B., Burnett, N. H. & Ivanov, M. Y. Subfemtosecond pulses. *Opt. Lett.* **19,** 1870–1872 (1994).
5. Eckle, P. *et al.* Attosecond angular streaking. *Nat. Phys.* **4,** 565–570 (2008).
6. Aeschlimann, M. *et al.* Coherent two-dimensional nanoscopy. *Science* **333,** 1723–1726 (2011).
7. Brixner, T. *et al.* Quantum control by ultrafast polarization shaping. *Phys. Rev. Lett.* **92,** 208301 (2004).
8. Hassan, M. T. *et al.* Optical attosecond pulses and tracking the nonlinear response of bound electrons. *Nature* **530,** 66–70 (2016).
9. Sommer, A. *et al.* Attosecond nonlinear polarization and light–matter energy transfer in solids. *Nature* **534,** 86–90 (2016).
10. Itatani, J. *et al.* Attosecond streak camera. *Phys. Rev. Lett.* **88,** 173903 (2002).
11. Kitzler, M., Milosevic, N., Scrinzi, A., Krausz, F. & Brabec, T. Quantum theory of attosecond XUV pulse measurement by laser dressed photoionization. *Phys. Rev. Lett.* **88,** 173904 (2002).

12. Kim, K. T. *et al*. Petahertz optical oscilloscope. *Nat. Photon.* **7,** 958–962 (2013).
13. Goulielmakis, E. *et al*. Direct measurement of light waves. *Science* **305,** 1267–1269 (2004).
14. Boge, R. *et al*. Revealing the time-dependent polarization of ultrashort pulses with sub-cycle resolution. *Opt. Express* **22,** 26967–26975 (2014).
15. Saliéres, P. *et al*. Frequency-domain interferometry in the XUV with high-order harmonics. *Phys. Rev. Lett.* **83,** 5483–5486 (1999).
16. Camper, A. *et al*. High-harmonic phase spectroscopy using a binary diffractive optical element. *Phys. Rev. A* **89,** 043843 (2014).
17. Lewenstein, M., Balcou, P., Ivanov, M. Y., L'Huillier, A. & Corkum, P. B. Theory of high-harmonic generation by low-frequency laser fields. *Phys. Rev. A* **49,** 2117–2132 (1994).
18. Sola, I. J. *et al*. Controlling attosecond electron dynamics by phase-stabilized polarization gating. *Nat. Phys.* **2,** 319–322 (2006).
19. Sansone, G. *et al*. Isolated single-cycle attosecond pulses. *Science* **314,** 443–446 (2006).
20. Sansone, G. Quantum path analysis of isolated attosecond pulse generation by polarization gating. *Phys. Rev. A* **79,** 053410 (2009).
21. Sansone, G. *et al*. Shaping of attosecond pulses by phase-stabilized polarization gating. *Phys. Rev. A* **80,** 063837 (2009).
22. Sansone, G., Benedetti, E., Vozzi, C., Stagira, S. & Nisoli, M. Attosecond metrology in the few-optical-cycle regime. *New J. Phys.* **10,** 025006 (2008).
23. Antoine, P., L'Huillier, A., Lewenstein, M., Saliéres, P. & Carré, B. Theory of high-order harmonic generation by an elliptically polarized laser field. *Phys. Rev. A* **53,** 1725–1745 (1996).
24. Paulus, G. G. *et al*. Measurement of the phase of few-cycle laser pulses. *Phys. Rev. Lett.* **91,** 253004 (2003).

Acknowledgements

This project has received funding from the European Union's Horizon 2020 research and innovation programme under the Marie Sklodowska-Curie grant agreement no. 641789 Molecular Electron Dynamics investigated by Intense Fields and Attosecond Pulses (MEDEA), the European Research Council Starting Grant agreement no. 637756 Steering attosecond electron dynamics in biomolecules with UV-XUV LIGHT pulses (STARLIGHT). Financial support by the Alexander von Humboldt Foundation (Project Tirinto) and the Italian Ministry of Research (project FIRB no. RBID08CRXK) is gratefully acknowledged.

A.C. acknowledges financial support from ENS Paris-Saclay. G.G.P. acknowledges support from the German Science Foundation (PA 730/7 within priority programme 1840).

Author contributions

P.C., M.R. and G.S. conceived and planned the experiment. P.C., M.R. and H.A. conducted the experiment. M.R. and A.C. analysed the data. S.K., F.C. and M.N. contributed to the development of the experimental set-up. L.P. and F.F. designed and installed the XUV beamline. D.H. and G.G.P. designed and installed the CE phase meter. J.U., C.D.S. and R.M. designed and installed the reaction microscope. G.S. performed the simulations and theoretical analysis. The manuscript was drafted by G.S. and completed in consultation with all the authors.

Additional information

Supplementary information is available in the online version of the paper. Reprints and permissions information is available online at www.nature.com/reprints. Publisher's note: Springer Nature remains neutral with regard to jurisdictional claims in published maps and institutional affiliations. Correspondence and requests for materials should be addressed to G.S.

Competing financial interests

The authors declare no competing financial interests.

Corrigendum: Vectorial optical field reconstruction by attosecond spatial interferometry

P. Carpeggiani, M. Reduzzi, A. Comby, H. Ahmadi, S. Kühn, F. Calegari, M. Nisoli, F. Frassetto, L. Poletto, D. Hoff, J. Ullrich, C. D. Schröter, R. Moshammer, G. G. Paulus and G. Sansone

Nature Photonics **11,** 383–389 (2017); published online 29 May 2017; corrected after print 29 June 2017.

In the version of this Article originally published, the following sentences were missing from the Acknowledgements: "Financial support by the Alexander von Humboldt Foundation (Project Tirinto) and the Italian Ministry of Research (project FIRB no. RBID08CRXK) is gratefully acknowledged. A.C. acknowledges financial support from ENS Paris-Saclay." These have now been added in the online versions of the Article.